Dielectric functions and critical points of $Be_xZn_{1-x}Te$ alloys measured by spectroscopic ellipsometry

M. R. Buckley and F. C. Peiris[a)]
Department of Physics, Kenyon College, Gambier, Ohio 43022

O. Maksimov, M. Muñoz, and M. C. Tamargo
Department of Chemistry, City College and Graduate Center of CUNY, New York, New York 10031

(Received 1 October 2002; accepted 6 November 2002)

Using a rotating analyzer spectroscopic ellipsometer, we have investigated the complex dielectric function of a series of ternary $Be_xZn_{1-x}Te$ thin films in the energy range between 0.7 and 6.5 eV for alloy concentrations between $x=0.0$ and $x=0.52$. After determining the alloy concentrations using x-ray diffraction and photoluminescence techniques, a standard inversion technique was used to obtain the optical constants from the measured ellipsometric spectra. Analyzing the second derivative of both the real and the imaginary parts of the dielectric constant, we have deduced the critical point parameters corresponding to the electronic transitions in the Brillouin zone. We find that the energy of the critical points with respect to Be concentration does not show any bowing effects unlike many other II–VI semiconductor ternary alloys. © *2002 American Institute of Physics.* [DOI: 10.1063/1.1534387]

Optoelectronic devices based on II–VI semiconductors containing beryllium have been recently proposed to overcome some of the conventional problems such as reduced life times and lower p-type doping concentrations that seem to effect most of the II–VI semiconductor devices. Beryllium incorporated II–VI crystals have been shown to form high degree covalent bonds, which give greater lattice hardening and lower degradation rates that are required in commercial applications.[1] Additionally, $Be_xZn_{1-x}Te$ can be p-doped to a level of 10^{19} cm^{-3} and also can be lattice matched to InP substrates which is advantageous for applications in lasers and light emitting diodes that operate in the visible wavelength range.[2,3] In order to fully exploit these materials as viable candidates for fabricating optical devices, their optical properties must be more completely cataloged. Very little knowledge of their optical properties is presently available, especially in the energy range above their band gap.

Spectroscopic ellipsometry is a powerful, nondestructive technique for determining the complex dielectric function $\epsilon = \epsilon_1 + i\epsilon_2$ of semiconductor thin films. Unlike many other experimental techniques, such as reflectivity measurements, ellipsometry eliminates the need for a Kramers–Kronig transformation. Using ϵ_1 and ϵ_2 obtained from ellipsometry, it is possible to easily calculate the index of refraction in the transparent region, which is of great interest when designing optoelectronic devices. In addition, observing the structure of ϵ_1 and ϵ_2 above the fundamental band gap E_0, one can identify higher order electronic transitions in the Brillouin zone and subsequently relate these to the band structure of the semiconductor alloys.

Previous work—which focused mainly on the optical properties in the transparent region—has categorized the band gap transitions of $Be_xZn_{1-x}Te$ alloys using a combination of reflectivity and photoluminescence measurements.[4] It was found that the $Be_xZn_{1-x}Te$ alloy family has a direct $\Gamma \rightarrow \Gamma$ band gap for $x<0.28$, while it becomes an indirect $\Gamma \rightarrow X$ band gap for $x \geqslant 0.28$. Furthermore, it was also reported that the E_0 critical point is linearly dependent upon Be content x, and can be described by the equation 2.26 eV $+(1.84\ \text{eV})x$.[4] In the present study, we extend the investigation of the optical properties of $Be_xZn_{1-x}Te$ alloys into the absorption region. Using a variable angle spectroscopic ellipsometer, the dielectric constant of a series of $Be_xZn_{1-x}Te$ II–VI semiconductor alloys was measured and the critical points in the Brillouin zone were identified.

The thin films were grown by molecular beam epitaxy (MBE) on semi-insulating epiready (001) InP substrates using a Riber 2300 MBE system. The substrates were dioxized at 500 °C under As flux, and a ~100-nm-thick, lattice matched InGaAs buffer layer was grown on the InP substrate. The growth temperature for the $Zn_{1-x}Be_xTe$ layer was maintained around 270 °C. The growth rate was approximately 0.5 μm/h, and $Be_xZn_{1-x}Te$ layers were 0.5–1.5 μm thick. No cap layer was necessary, as no surface degradation of this material has been observed even over extended periods of time. Fifteen samples of $Be_xZn_{1-x}Te$ alloys were grown for this study, with Be concentrations (x) ranging from $x=0$ to $x=0.516$. The composition of the films was determined using single-crystal x-ray diffraction, assuming a linear dependence of the lattice constant with respect to the alloy concentration. The spectroscopic analysis was performed using a Woollam ellipsometer, capable of taking ellipsometric data with photon energies of 0.7–6.5 eV. For each sample we obtained room temperature ellipsometric data at angles of incidence of 65°, 70°, and 75°.

In standard ellipsometry, two parameters, ψ and Δ, are measured at each wavelength for a particular sample. ψ and Δ are related to the ratio of reflection coefficients by

$$\rho = \frac{R_p}{R_s} = \tan(\psi) e^{i\Delta},$$

a)Electronic mail: peirisf@kenyon.edu

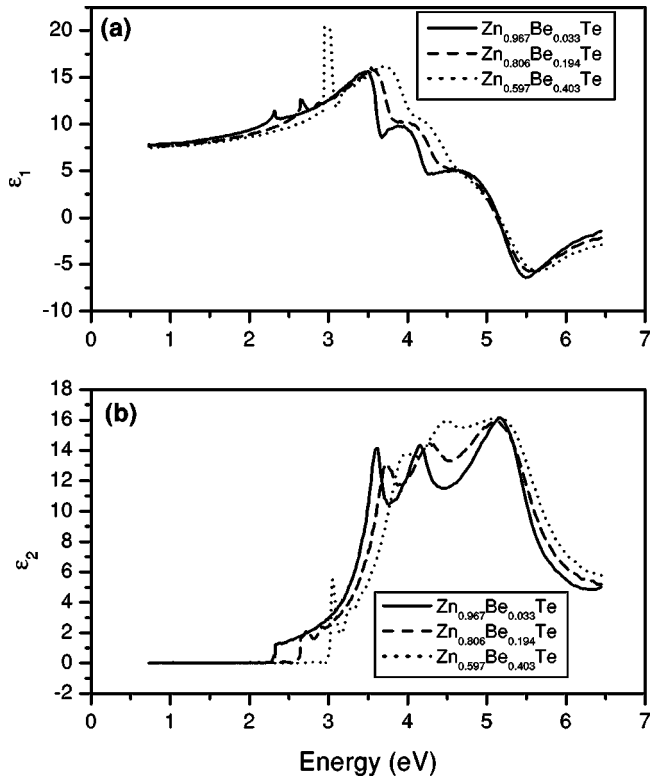

FIG. 1. The (a) real (ϵ_1) and (b) imaginary (ϵ_2) components of the dielectric function of three representative samples of $Zn_{1-x}Be_xTe$.

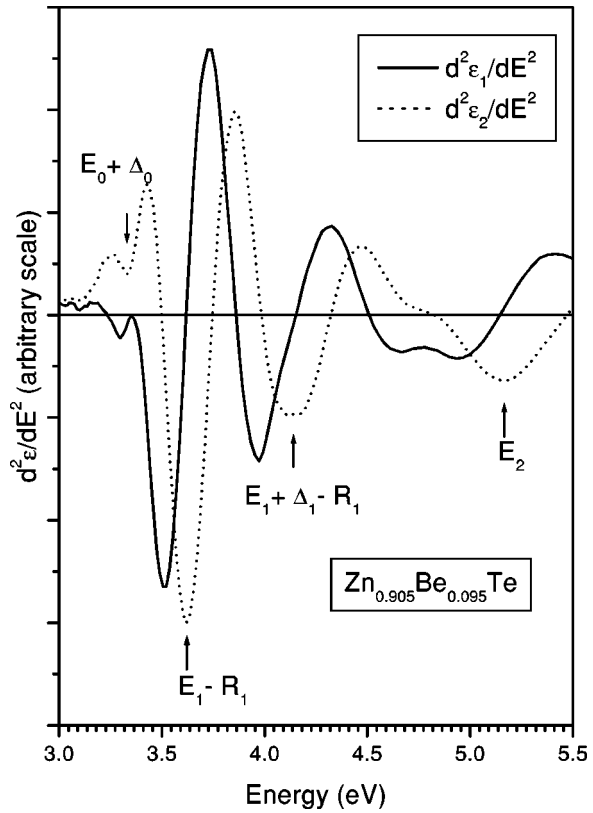

FIG. 2. The second derivative with respect to energy of ϵ_1 and ϵ_2 for $Zn_{0.905}Be_{0.095}Te$ with the zero line given as a reference. The position of the transitions $E_0+\Delta_0$, E_1-R_1, $E_1+\Delta_1-R_1$ and E_2 are noted.

where R_p is the complex reflection coefficient for light polarized parallel to the plane of incidence, and R_s is the coefficient for light polarized perpendicular to the plane of incidence. As ψ and Δ depend on the optical properties for the entire semiconductor, a four layer model (i.e., InP substrate, InGaAs buffer, $Be_xZn_{1-x}Te$ layer, and surface oxide layer) was constructed for each sample to determine the optical properties of the $Be_xZn_{1-x}Te$ layer. As the optical properties of the substrate, buffer, and oxide are already known,[5] the thicknesses of each layer and the optical properties of the $Be_xZn_{1-x}Te$ layer were adjusted to match the experimental data. This was achieved in two steps. First, focusing only on the ψ and Δ spectra obtained in the transparent region, the optical properties in the transparent region (i.e., below the fundamental E_0 band gap) of $Be_xZn_{1-x}Te$ layer were approximated using a Cauchy model. This allowed us to accurately determine the index of refraction n and the extinction coefficient k of the $Be_xZn_{1-x}Te$ layer in the transparent region, as well as to obtain the thicknesses of all four layers.[6] After the individual layer thicknesses and the transparent region optical properties of $Be_xZn_{1-x}Te$ were determined, the next step was to simulate the above band gap optical properties of $Be_xZn_{1-x}Te$ to give the best fit to the experimental ψ and Δ spectra. The components of the complex dielectric function, ϵ_1 and ϵ_2, determined from this procedure are plotted in Fig. 1 for representative samples of $Be_xZn_{1-x}Te$ over the measured photon energy range. From Fig. 1, one immediately recognizes that the incorporation of Be into the lattice blueshifts the energy gap in the $Be_xZn_{1-x}Te$ alloy system. Furthermore, as seen from Fig. 1(a), the samples with higher Be concentration show a distinct peak at the onset of absorption which we believe is due to excitons in the $Be_xZn_{1-x}Te$ alloys.[7,8] The presence of a room temperature exciton near E_0, as seen from Fig. 1(a), indicates the high quality of the crystalline structure. This has been confirmed by the fact that both the x-ray and photoluminescence data show very narrow peaks for these particular $Be_xZn_{1-x}Te$ thin films.[9]

To determine the correct energy position of the critical points (CPs) associated with the electronic transitions in the Brillouin zone (i.e., E_0, $E_0+\Delta_0$, E_1, $E_1+\Delta_1$, and E_2), we use the second derivatives of ϵ_1 and ϵ_2 with respect to energy.[10–12] In Fig. 2 we show typical plots of $d^2\epsilon_1/dE^2$ and $d^2\epsilon_2/dE^2$ obtained for a representative sample of the $Be_xZn_{1-x}Te$ alloy family. The second derivatives of the dielectric function for $Be_{0.095}Zn_{0.905}Te$ shown in Fig. 2 indicate that the energy of the CPs can be assigned unambiguously from this method. We note that since the excitonic effects dominate near the E_1 and $E_1+\Delta_1$ CPs, one can only determine the CP energies minus the binding energy (R_1) from this method.[8,13] A detail study of the second derivative spectral characteristics is currently underway to determine the excitonic behavior in the $Be_xZn_{1-x}Te$ alloy system. In addition, competing models[8,14,15] are also studied in order to extract the binding energies and some of the other parameters from the dielectric function.

The energy positions of the CPs determined from analyzing the second derivatives are shown in Fig. 3. The positions are shown as a function of Be concentration, along with their best linear fits represented by dotted lines. The linear fits obtained for each of the CPs as a function of Be concentration are reported in Table I. It must be noted that the linear fit obtained for E_0 transition from this present work is consistent with reflectivity and photoluminescence results previ-

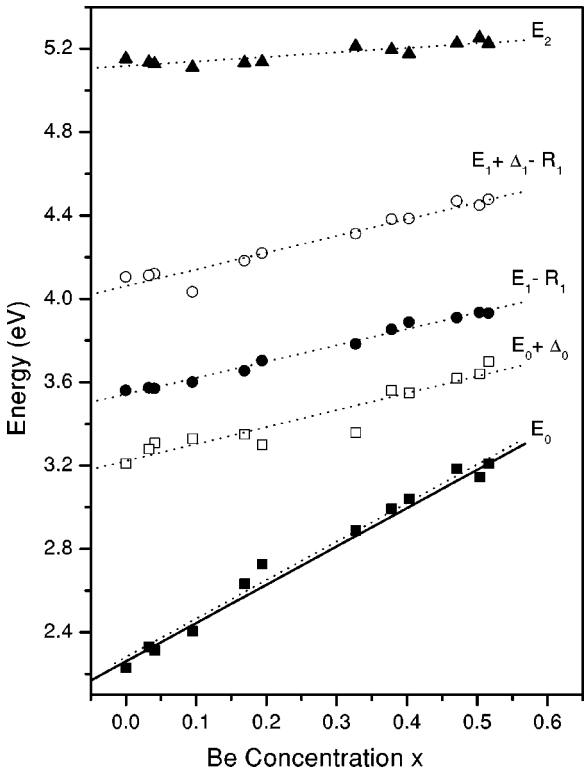

FIG. 3. The position of the transitions as a function of Be concentration. The E_0 (filled squares), $E_0+\Delta_0$ (open squares), E_1-R_1 (filled circles), $E_1+\Delta_1-R_1$ (open circles), and E_2 (filled triangles) transitions are plotted, along with their linear fits which are indicated by dotted lines. The parameters associated with the linear fits are presented in Table I. Note the solid line associated with the E_0 transition is the data taken from Ref. 4 which was obtained using reflectivity and photoluminescence measurements.

ously reported for the $Be_xZn_{1-x}Te$ alloy system.[4] This is shown as a solid line associated with the E_0 transition in Fig. 3. It is also interesting to note the absence of any bowing effects in all of the CPs with respect to the alloy concentration in $Be_xZn_{1-x}Te$. This is in contrast to most of the other II–VI semiconductor ternary alloys such as $Cd_xZn_{1-x}Se$,[16] $Mg_xZn_{1-x}Se$,[11] and $Be_xZn_{1-x}Se$[11,17] which all exhibit some degree of bowing in all of their CPs. However, it is striking that similar to $Be_xZn_{1-x}Te$ alloys in which the Te appears as the anion, $Cd_xMn_{1-x}Te$ alloys also show a linear behavior of its CPs with respect to the alloy concentration.[18]

Previous studies of the binary compound ZnTe have relied upon chemical etching procedures to eliminate surface irregularities that could influence the ellipsometric results.[14] However, by adding a surface oxide layer to our semiconductor model, we were able to circumvent the need for such surface treatments.[7] The modeled oxide layer used optical constants that were an average between that of air and the $Be_xZn_{1-x}Te$ layer beneath. It must also be mentioned that the thin films used in this study were relaxed as their thicknesses exceeded the critical thickness for strain relaxation.[19] Hence, we expect that the dielectric constants calculated for our thin films of $Be_xZn_{1-x}Te$ to be essentially that of bulk $Be_xZn_{1-x}Te$.

TABLE I. Values of the parameters (a) and (b) associated with the fits obtained for the transition points. The transition point energy vs Be concentration (x) was fitted to the linear equation $E=ax+b$.

Transition	a (eV)	b (eV)
E_0	1.85 ± 0.08	2.28 ± 0.02
$E_0+\Delta_0$	0.81 ± 0.03	3.22 ± 0.01
E_1-R_1	0.78 ± 0.03	3.54 ± 0.01
$E_1+\Delta_1-R_1$	0.80 ± 0.03	4.06 ± 0.01
E_2	0.22 ± 0.03	5.12 ± 0.01

In summary, we have used a spectroscopic ellipsometer to measure the dielectric constant of a series of molecular beam epitaxy-grown $Be_xZn_{1-x}Te$ alloys. Most of the room temperature ellipsometric spectra obtained for these samples show the presence of excitons which attest to the high quality of the specimens. The critical points related to the $Be_xZn_{1-x}Te$ alloys were obtained by taking the second derivatives of the dielectric constant with respect to the energy. Unlike most other II–VI semiconductor alloys, all of the critical points obtained for the $Be_xZn_{1-x}Te$ alloy system show no bowing effects with respect to the alloy concentration.

The authors wish to thank Corey Bungay and Professor John Woollam for fruitful discussions, and also Professor Timothy Sullivan for valuable suggestions.

[1] G. Landwehr, F. Fischer, T. Baron, T. Litz, A. Waag, K. Schüll, H. Lugauer, T. Gerhard, M. Keim, and U. Lunz, Phys. Status Solidi B **202**, 645 (1997).
[2] S. B. Che, I. Nomura, W. Shinozaki, A. Kikuchi, K. Shimomura, and K. Kishino, J. Cryst. Growth **214**, 321 (2000).
[3] M. W. Cho, S. K. Hong, J. H. Chang, S. Saeki, M. Nakajima, and T. Yao, J. Cryst. Growth **214/215**, 487 (2000).
[4] O. Maksimov and M. C. Tamargo, Appl. Phys. Lett. **79**, 782 (2001).
[5] C. Pickering, R. T. Carline, M. T. Emeny, N. S. Garawal, and L. K. Howard, Appl. Phys. Lett. **60**, 2412 (1992).
[6] C. M. Herzinger, P. G. Snyder, F. G. Celii, Y.-C. Kao, D. Chow, B. Johs, and J. A. Woollam, J. Appl. Phys. **79**, 2663 (1996).
[7] H. C. Ong and R. P. H. Chang, Appl. Phys. Lett. **79**, 3612 (2001).
[8] T. Holden, P. Ram, F. H. Pollak, J. L Freeouf, B. X. Yang, and M. C. Tamargo, Phys. Rev. B **56**, 4037 (1997).
[9] O. Maksimov, Ph.D thesis, City College and Graduate Center of CUNY, 2001.
[10] P. Lautenschlager, M. Garriga, L. Viña, and M. Cardona, Phys. Rev. B **36**, 4821 (1987).
[11] H. Lee, I. Kim, J. Powell, D. E. Aspnes, S. Lee, F. Peiris, and J. K. Furdyna, J. Appl. Phys. **88**, 878 (2000).
[12] Y. D. Kim, S. G. Choi, M. V. Klein, D. S. Yoo, D. E. Aspnes, S. H. Xin, and J. K. Furdyna, Appl. Phys. Lett. **70**, 610 (1997).
[13] M. Muñoz, K. Wei, F. H. Pollak, J. L. Freeouf, and G. W. Charache, Phys. Rev. B **60**, 8105 (1999).
[14] K. Sato and S. Adachi, J. Appl. Phys. **73**, 926 (1993).
[15] M. Muñoz, F. H. Pollak, M. Kahn, D. Ritter, L. Kronik, and G. M. Cohen (unpublished).
[16] Y. D. Kim, M. V. Klein, S. F. Ren, Y. C. Chang, H. Luo, N. Samarth, and J. K. Furdyna, Phys. Rev. B **49**, 7262 (1994).
[17] K. Wilmers, T. Wethkamp, N. Esser, C. Cobet, W. Richter, M. Cardona, V. Wagner, H. Lugauer, F. Fischer, T. Gerhard, and M. Keim, Phys. Rev. B **59**, 10071 (1999).
[18] P. Lautenschlager, S. Logothetiidis, L. Vina, and M. Cardona, Phys. Rev. B **32**, 3811 (1985).
[19] J. W. Matthews and A. E. Blakeslee, J. Cryst. Growth **27**, 118 (1974).